Food and Bioprocess Technology (2023) 16:3057–3072
https://doi.org/10.1007/s11947-023-03119-9

RESEARCH

Insights into the FTIR Spectral Fingerprint of Saffron (*Crocus sativus* L.) Stigmas After Gentle Drying Treatments

Fotini Kokkinaki[1] · **Stella A. Ordoudi**[1,2]

Received: 26 February 2023 / Accepted: 4 May 2023 / Published online: 20 May 2023
© The Author(s) 2023

Abstract

Drying of the delicate, red stigmas of the *Crocus sativus* L. flower is necessary to produce saffron, the most expensive spice in the world. So far, laborious and sample destructive methods were applied to get vital insight into this process following key physicochemical changes. Vibrational spectroscopy tools that allow molecular fingerprinting of plant tissues via multivariate data analysis are still not exploited. This study aimed at gaining new insights into the Fourier-Transform Infrared (FTIR) spectra of saffron on different gentle drying treatments in vacuum or by short-time heating with varying sample loading, energy input, duration etc. Diagnostic spectral bands that were exposed using Principal Component Analysis were assigned to C=O stretching in vinyl or cyclic esters, amides or other inter-molecular interactions of importance for functionality. Above all, the peak at 1160 cm^{-1} (typical of C-O-C glycosidic bridges) proved a distinguishing feature of short-time heated vs vacuum-dried saffron. Other critical quality attributes of the dried stigmas (physical structure, color, chemical composition), assessed with Scanning Electron Microscopy (SEM), colorimetry, UV-Vis spectrometry and High-Performance Liquid Chromatography (HPLC), indicated both positive and negative effects per drying method. Our work highlights the novelty to combine non-destructive FTIR spectroscopy with conventional techniques for a more insightful evaluation of desired or undesired changes after saffron dehydration. Moreover, the spectral fingerprinting approach offers a cost-effective, eco-friendly solution for rapid, non-invasive control of the raw material that is of high interest for food and nutraceutical applications.

Keywords Saffron quality · Crocetin sugar esters · Picrocrocin · Drying · FTIR spectroscopy

Introduction

Saffron, a spice of high economic importance in several Asian and European producing countries, is well appreciated in the global food market for its elegant coloring and flavoring properties. It refers to the delicate red stigmas of the *Crocus sativus* L. flower that are manually collected, sorted, and dried before packaging and trade. Thermal treatment is necessary to tackle safety issues and to prolong the shelf-life of the stigmas while it may differentiate the compositional profile of the final product. In Europe, traditional hot air-drying processes in the major producing regions (Greece, Italy, Spain) are indorsed via Protected Designation of Origin (PDO) labels and specifications that provide added value to the local products (Carmona et al., 2006a). Even so, alternative, greener practices using non-conventional or nonthermal technologies are gaining interest in the last years (Majumder et al., 2021). Gentle vacuum-drying, short-time heating with microwaves, and thin-layer drying above a "refractance window" are some of the novel techniques that were suggested in view of upscaling and modern industrial applications of saffron (e.g., Acar et al., 2015; Aghaei et al., 2018; Chen et al., 2020; García-Blázquez et al., 2021).

Over the years, several researchers investigated the effects of traditional drying methods and proposed optimal conditions to retain high organoleptic quality of this product. Major secondary metabolites comprising various sugar esters of crocetin, an orange-yellow C20 apocarotenoic acid, along with picrocrocin, a bitter monoterpene glucoside, and certain aroma-active terpenoids (e.g., safranal) that are formed upon

✉ Stella A. Ordoudi
steord@chem.auth.gr; stella.ordoudi@gmail.com

[1] Laboratory of Food Chemistry and Technology (LFCT), School of Chemistry, Aristotle University of Thessaloniki, 54124 Thessaloniki, Greece

[2] Natural Products Research Center of Excellence (NatPro-AUTH), Center for Interdisciplinary Research and Innovation (CIRI-AUTH), Aristotle University of Thessaloniki, 57001 Thessaloniki, Greece

stigma dehydration gained the greatest attention (Carmona et al., 2006c; Gregory et al., 2005; Kanakis et al., 2004). These metabolites are also important for antioxidant and other bio-functions of the spice (Kyriakoudi et al., 2015). Today, there is a gap in knowledge about the drying effects on other classes of constituents (e.g., carbohydrates, amino acids, proteins, lipids, and minerals) with possible implications to organoleptic or bio-functional properties of saffron.

Thus far, various methods with laborious, time-consuming protocols that require expensive instrumentation and high technical expertise were used to evaluate the dehydration effects on saffron quality. In the last decade, non-destructive vibrational spectroscopy techniques (e.g., near-, mid-infrared (NIR, MIR), Raman, or hyperspectral imaging) coupled with chemometrics were proposed for rapid saffron authentication and forensic analyses (e.g., Amirvaresi et al., 2021; Ordoudi et al., 2018; Petrakis et al., 2017; Zalacain et al., 2005) or evaluation of ageing effects (Ordoudi et al., 2014) indicating a strong potential of fingerprinting analyses. Nevertheless, mid-infrared spectroscopy may offer an additional asset in investigating molecular structural changes at the last stage of dehydration (Hassoun et al., 2021; Ren et al., 2022) when spectral interference from the remaining water is likely reduced to a minimum degree (Ren et al., 2022). Through spectral fingerprints, it is possible to obtain rapidly insightful information about different molecular interactions and pinpoint features of possibly diagnostic value about the product quality. Regarding saffron, this piece of valuable information is generally lacking.

The present study aimed at gaining new insights into the Fourier transform infrared (FTIR) spectra of saffron stigmas on various drying patterns that involved vacuum or short-time heating at different operating conditions (sample loading, pressure, microwave energy, duration, etc.). The primary goal was to expose diagnostic bands per different drying method that would help to understand key molecular structure transformations and evaluate their association with desired or undesired changes in key quality attributes. Additionally, the physical structure and color along with chemical constituents of high organoleptic value were assessed via conventional analytical methods (scanning electron microscopy (SEM), colorimetry, UV-Vis spectrometry, and high-performance liquid chromatography (HPLC)). To our knowledge, this is the first time that an FTIR spectroscopic fingerprinting approach is exploited as an alternative method for thorough investigation of quality changes after saffron dehydration by different techniques.

Materials and Methods

Standards, Reagents, and Solvents

Trans-crocetin di-(β-D-gentiobiosyl) ester (trans-4-GG) and picrocrocin of RP-HPLC-DAD purity (> 95%) were laboratory-isolated from saffron aqueous extract using a preparative reversed-phase high-performance liquid chromatography (RP-HPLC) SpectraSYSTEM apparatus and a diode array detector on a Sigma-Aldrich Fortis C18, 100 Å, (250 × 21.2, 2 μm). The elution protocol and identification conditions are given in Online Resource 1. HPLC-grade methanol was from Chem-Lab (Zedelgem, Belgium). Ultra-high-purity water was produced using a SG Ultra Clear Basic UV system (SG Wasseraufbereitung und Regenerierstation GmbH, Barsbüttel, Germany). FTIR-grade KBr (> 99%) was purchased from Sigma-Aldrich (Steinheim, Germany).

Saffron Samples

Fresh stigmas from full-bloom flowers of the *Crocus sativus* L. plants were collected from a single field (organic) in the region of Kozani (North-Western Greece) (40°11′20.9″N 21°48′27.6″E). After picking the flowers, around 3 kg of red stigmas were first-hand sorted from petals and stamens and a portion was kept for drying (35 °C, ca. 60% air humidity, 12 h) until a residual moisture of 10 – 11% w/w, according to the traditional process (Ordoudi & Tsimidou, 2004). The remaining amount of fresh material was packed in food-grade plastic bags, sealed in cool condition (< 5 °C) and transported within 2 h in the Laboratory of Food Chemistry and Technology, Thessaloniki, Greece, for further processing of the perishable stigmas. The time elapsed after harvest was between 4 – 5 h. Floral waste and soil, insects, etc. were carefully removed from the fresh material. The cleaned stigma sample was split in equal portions of around 80 g; sealed in food-grade, water barrier bags; and stored at – 20 °C until the vacuum-drying treatment or exposed to short-time drying experiments within the same day.

Dehydration Experiments

The experimental drying protocols and operating conditions that were followed to prepare freeze-dried (FD), vacuum oven-dried (VOD), microwave oven-dried (MWD), and refractance window-dried (RWD) saffron are explained in detail in Online Resource 2. The stigmas were removed when they lost 80 ± 2% of their weight (wet basis). Table 1 lists the test samples that were produced from different dehydration experiments.

Physicochemical Characterization of Dry Stigmas

Residual Moisture and Volatile Content Determination

Residual moisture of the dry stigma samples (H, % w/w) was determined in duplicate using the gravimetric method proposed in ISO 3632-2:2010 (ISO, 2010).

Table 1 Experimental saffron samples after dehydration with different gentle drying processing

Sample code (no of replicates)	Physical state of stigmas	Instrumentation	Duration (h)	Sample loading	
				Oven or chamber (g/L)	Tray (g/m^2)
FD1-4 ($n=4$)	Frozen	Freeze-dryer	4	14 – 15	400 – 600
FD1-9 ($n=4$)	Frozen	Freeze-dryer	9	14 – 15	400 – 600
FD1-24 ($n=4$)	Frozen	Freeze-dryer	24	14 – 15	400 – 600
FD2-4 ($n=4$)	Frozen	Freeze-dryer	4	6 – 7	400 – 600
FD2-9 ($n=4$)	Frozen	Freeze-dryer	9	6 – 7	400 – 600
VOD-9 ($n=2$)	Frozen	Vacuum oven (30 °C)	9	< 3.9	400 – 700
VOD-20 ($n=2$)	Frozen	Vacuum oven (30 °C)	20	< 3.9	400 – 700
MWD1-5 ($n=5$)	Wet	Microwave oven (360 W)	0.05 – 0.17		300 – 950
MWD1-5 ($n=5$)	Wet	Microwave oven (540 W)	0.05 – 0.17		300 – 950
RWD1-7 ($n=7$)	Wet	Polyester film-water bath (90 °C)	0.38 – 0.49		300 – 900

Microstructure and Color Analyses

Surface morphology of the whole stigmas was observed under scanning electron microscope (JEOL, JMS-840) (Interdisciplinary Laboratory of Electron Microscopy, AUTh, Greece). A stigma sample was coated with carbon black to avoid charging under the electron beam and viewed under accelerated voltage of 21 kV and probe current of 45 nA. Surface color was objectively measured with the aid of a portable HunterLab spectrophotometer (MiniScanTM XE Plus, Reston, VA, USA) and with reference to the D65 illuminant source and the 10◦ Observer. The dried stigmas were placed on a magnetic white ceramic disk on the face of a clamp that provides a consistent white background for reflectance measurements. The data were automatically transformed according to the CIELAB color system, so that tristimulus coordinate L, a*, and b* values, expressing lightness (L*), variation between red/green (positive vs. negative a* values), or yellow/blue color (positive vs. negative b* values), were recorded. Chroma (C*) that represents color saturation or intensity and hue angle (h^o) that describes the relative amounts of redness and yellowness were calculated from a* and b* values according to the following formulae.

$$Chroma\,(C^*) = \sqrt{(a^{*2} + b^{*2})} \tag{1}$$

$$Hue\ angle\,(h^o) = \tan^{-1}({}^{b^*}/_{a^*}) \tag{2}$$

The increase of hue angle value from 0 to 90° indicates a shift from red to orange-yellow color.

Polar Extract Preparation

Saffron stigmas were ground in a pestle mortar and passed through a sieve of 0.5-mm mesh, following the crushing and sieving method proposed in ISO 3632-2:2010 (ISO, 2010). Methanol-water extracts of ground stigmas were prepared as follows. An amount of 0.1 g was transferred in a 200-mL volumetric flask and mixed with methanol-water (1:1, v/v) up to the mark. Water-soluble colored and non-colored constituents were extracted by rigorous agitation (1000 rpm) for 1 h at ambient temperature (25 °C) away from direct sunlight. Prior to analysis, an aliquot from the extract was diluted (1:10) with the solvent mixture and the corresponding solutions were filtered through a PVDF filter (0.45-um pore size, Millipore, Bedford, MA).

UV-Vis Spectrophotometric Examination

The UV-Vis spectra of methanol-water extracts were recorded in the region 200–600 nm using the Shimadzu UV 1601 (Kyoto, Japan) and processed with the aid of UVPC 1601 (Personal Spectroscopy Software, v.3.9, Shimadzu) software facilities. Spectral characteristics that are considered indices of coloring strength, bitterness, and aroma strength of the spice (associated with the total content in crocetin sugar esters, picrocrocin, and safranal, respectively) were calculated, on a dry basis, according to the ISO3632-2:2010 method using the following equation:

$$E^{1\%}_{\lambda max} = (D \times 10000)/(m \times (100 - H)) \tag{3}$$

with D as the absorbance value, m as the mass of the test portion (g), H as the moisture, and volatile content of the sample (%, w/w) was used; λmax for crocetin sugar esters, 440 nm, λmax for picrocrocin, 257 nm; and λmax for safranal, 330 nm. The reported values are the average values of two replicates.

HPLC-DAD Analyses of CRTSEs and Picrocrocin

The composition of methanol-water saffron extracts in polar apocarotenoids (CRTSEs, picrocrocin) was investigated as follows. The test metabolites were separated on a Synergi™ Max-RP 80 Å (150 × 4.6 mm i.d, 4 µm) C12 column with TMS endcapping (Phenomenex, CA, USA) after injection of a 20-mL aliquot and gradient elution with a mixture of water (A) and methanol (B) (30 to 100% B in 30 min) at a flow rate of 0.5 mL min^{-1}. A Shimadzu Nexera X2 UHPLC System (Shimadzu Corporation, Kyoto, Japan), equipped with a SIL-30AC autosampler, a CTO-20AC column oven, and a UV/visible diode array SPD-M30A detector (DAD) was used. Data acquisition and analysis were carried out using Lab Solution ver. 5.86 software (Shimadzu Corporation, Kyoto, Japan). Column temperature was maintained at 30 °C and that of the sample at 10 °C. Chromatograms were recorded at 440 nm and 250 nm. Peak identification was based on the available standards, relative retention times, spectra matching, and the literature (Carmona et al., 2006c). Quantification of total CRTSEs and picrocrocin (%, w/w on a dry basis) was accomplished with the aid of external standard calibration curves using stock methanolic solutions of *trans*-4-GG and picrocrocin in the range of 34–112 ng ($R^2 = 0.999$, $n = 6$, LOQ = 5.51 ng) and 13 − 130 ng ($R^2 = 0.999$, $n = 5$, LOQ = 1.59 ng), respectively. The limit of quantification (LOQ) was calculated as $10 \times \sigma/S$ where σ is the standard deviation of the y-intercept and S is the slope of the calibration curve.

FTIR Spectroscopic Fingerprinting

Acquisition of FTIR Spectra

The mid-infrared vibrational spectra of the dried samples were recorded using a Fourier transform infrared (FTIR) spectrometer (Shimadzu IRAffinity 1, Kyoto, Japan) in transmission mode and evaluated by the method described by Ordoudi et al. (2014). The absorbance spectrum from 4000 to 600 cm^{-1} was obtained with a number of 64 scans at a resolution of 4 cm^{-1} using the software provided by the manufacturer (Shimadzu IRSolution, Kyoto, Japan).

Data Preprocessing and Principal Component Analysis

The spectra were first corrected for signals of CO_2 and water and then smoothed by 15 points using the IRSolution software functions ‘‘atmosphere correction” and “smoothing action,” respectively. The processed data were exported as JCAMP (Joint Committee on Atomic and Molecular Physical) data (.dx) and merged with the aid of the SIMCA 16.1 software (Umetrics, Umeå, Sweden) to generate a pooled data matrix of N (samples) × K (instrumental response at each wavenumber) dimensions in a row-wise direction. Two different working data sets were created after (a) normalization through the standard normal variate method (SNV) and (b) normalization (SNV) and 2nd-order derivatization through Savitzky-Golay method and 11 interval points. Data from the spectral regions among 1800 − 2600 and 3600 − 4000 cm^{-1} were devoid of signals and, thus, excluded, while the rest ($K = 1245$) were mean centered (all signal responses across a column are converted to fluctuations around the mean value) and analyzed via the Principal Component Analysis (PCA) algorithm encoded in the SIMCA© 16.1 software (Umetrics, Umeå, Sweden). The results were evaluated by assessing the covariance of the new multidimensional data to select the number of “significant” PCs. Selection was according to the total variance explained (> 95% cumulative variation) and/or fitness to the Kaiser criterion (all components with eigenvalues greater than 1.0). The PCA scoreplots were inspected for similarity/difference patterns in the spectral data. Variable loading plots were carefully explored to identify significant spectral features (absolute p loading > 0.05) that are of biochemical relevance. The reduced distance rule was used to evaluate extreme values or possible outliers of the PC-modelled spaces (Ordoudi et al., 2022).

Results and Discussion

Freshly collected stigma of Greek origin, which represents also the major domestically cultivated saffron product in Europe, was used in this study, as base material for the drying treatments. The reference sample followed drying specifications of the Protected Designation of Origin (PDO) “Krokos Kozanis” product, that is, gentle heating of stigma in thin layers over varying tray dimensions and sample loads until a deep red color and brittle texture are attained (Ordoudi & Tsimidou, 2004). The test samples represented two alternative patterns of gentle drying. The first involved vacuum-drying through pre-freezing and lyophilization (freeze-drying, FD) or heating at 30 °C (vacuum oven-drying, VOD) over a period of 4 − 24 h. The second was about short-time heating (3 − 30 min) at < 70 °C, mediated

by microwave (MW) or through an infrared refractance window (RW).

Drying Yields and Critical Process Variables

In most kinds of spices, the last stage of dehydration that represents the second falling drying rate period is dominated initially by liquid diffusion of moisture followed by vapor diffusion with further progress (Majumder et al., 2021). To examine whether FTIR spectroscopy can highlight dynamic changes at this stage, we performed drying experiments with increasing sample loading in association with other operating parameters that differentiated the drying rate of saffron. It is stressed that so far, the effects of stigma loading and density on the drying kinetics or quality characteristics of saffron are underexplored. Nevertheless, in our study, the stigmas were removed on a weight loss of $80 \pm 2\%$ w/w. Their residual moisture content ranged widely between 5.4 and 12.2%, regardless of the drying method but strongly depending on the operating conditions (Online Resource 4). For example, both loading and duration of FD experiments proved critical for obtaining samples with low moisture contents that were considered safe for storage at ambient temperature (Tsimidou & Biliaderis, 1997) and acceptable for further analyses. Variation in several other instrumental parameters, e.g., pre-freezing temperature, pressure, and shelf temperature gradient, could be more relevant in future optimization studies. Vacuum-oven drying at the set temperature, pressure, and sample loading conditions progressed rather slowly so that extending the duration of the process was important to obtain drier samples. In the case of microwave-oven drying, increased sample loading (from MWD1 to MWD5) under low to medium power intensity conditions (360, 540 W) differentiated the MW energy input, while higher loads resulted in rather drier samples. On the contrary, drying over an in-house "refractance window" dryer (Online Resource 3) required relatively low load and density of thin stigma layers as in samples RWD4-7.

Physical Characteristics of Dry Stigmas

Microstructure

The shrinkage level and the internal void structure that are associated with the grinding ability of dried plant products were evaluated here as a result of different gentle drying treatments of saffron. The FD samples seemed to preserve the original shape of the fresh, non-dried stigmas in line also with previous findings (Chen et al., 2020). However, the SEM photographs of the surface structure revealed severe cracks and irregular particles with indentation as those shown in Fig. 1a–c for FD1-9. Such drastic deformations denote that the conjunctive tissue in cellular structures was lost which may explain why the number of pollen grains was significantly reduced, when compared with traditionally air-dried CS (Fig. 1m–o). Saffron pollen may contain bioactive terpenoids that could be desirable for consumption (Chia-Ying & Tian-Shung, 2002). In contrast, VOD stigmas (Fig. 1d–f) retained uniform structures. The VOD stigmas appeared more shrunken than FD, as also evidenced by other researchers (Chen et al., 2020). In this case, the pollen grains were trapped in the papillae retaining their globular shape and resisting detachment (Fig. 1e).

Shorter duration and faster moisture transfer are expected to restrict structural collapse and form a more porous structure. Short-time heating treatment with microwaves (Fig. 1g–i) resulted in a characteristic puffing effect on the upper part of the stigma due to higher internal void structure (Fig. 1g). During MW drying, the generation of internal heat vaporizes the unbound water which rapidly flows up to the surface creating a porous structure in the inner core (Majumder et al., 2021). As a consequence, MWD saffron were less shrunken and less abundant in pollen grains than CS. The remaining grains retained their spherical scheme and conjunction with the stigma tissue. On the other hand, drying over a refractance window did not alter the appearance and texture of stigmas, compared with traditionally air-dried CS. RWD samples brought loose, porous, less shrunk, and nearly devoid of pollen grains structures (Fig. 1j–l vs m–o). It has been suggested that the thin-layer RW heating conditions induce a massive stress to the microstructure of the samples due to the rapid mass transfer that may cause vapor saturation of the surrounding air and hinder product exposure to oxygen (Nindo & Tang, 2007). Another view could be that an outer "glassy" layer that is formed due to the rapid decrease in moisture content hinders cell collapse and shrinkage of the plant stigma (Aguilera, 2003; Majumder et al., 2021).

Summing up, gentle drying treatments differentiated the microstructural characteristics of the stigma surface bringing about undesired structural collapse (freeze-drying), creating inner porous structure or outer glassy surface with partial detachment of pollen grains (microwave oven and refractance window), or retaining more uniform structure and conjunctive tissue (vacuum-oven drying).

Surface Color Attributes

Figure 2 shows the values of the CIELab color space coordinates that represent lightness (L), redness (+a*), and yellowness (+b*) together with overall brightness or saturation (C*) and hue angle (h^o) of the color of stigmas from different drying treatments, in comparison to those of traditionally air-dried saffron (CS). At a first sight, all the test samples were nearly as bright as CS ($L^* < 30$). Stigmas dried in vacuum (FD and VOD) were lighter in color than those dried at

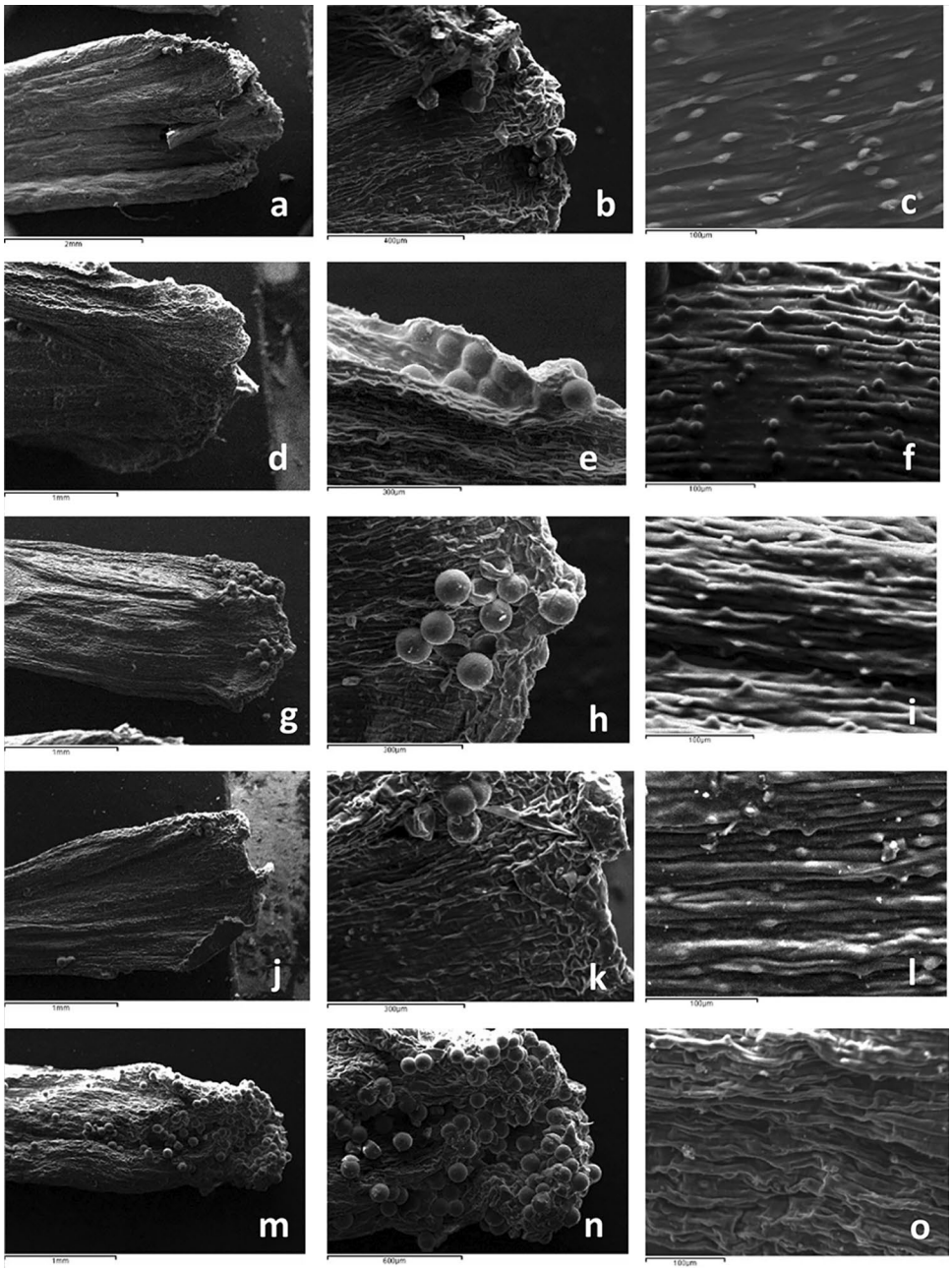


Fig. 1 SEM micrographs of selected whole stigmas after **a–c** freeze-drying (FD1-9); **d–f** vacuum-oven drying (VOD-9); **g–i** microwave-oven drying (MWD5-540); **j–l** refractance window-drying (RWD-7); **m–o** traditional air-drying (control, CS). Scales vary from left to right column: 1 – 2 mm, 300 – 600 μm, and 100 μm

higher temperatures in the presence of oxygen (MWD and RWD), which implies that non-enzymatic browning reactions may have taken place in the latter conditions.

FD stigmas exhibited red to orange color (C* = 17 – 35, $h = 29 - 42°$) that turned more yellowish and atypical of saffron-like appearance over an extended period of drying (FD1-24, FD2-9). FD1-9 was the brightest in color (Fig. 2). In the relevant study of Chen et al. (2020) the FD stigmas retained a much brighter red–orange color (L* = 53.1, C* = 51.5, $h = 36.9°$), probably due to different FD operating conditions, part of the plant tissue tested and/or geographical origin of saffron. In contrast to FD and air-dried CS, saffron samples after either 9 or 20 h of VOD treatment attained dull dark red color, as depicted by lower C* and hue angle values in Fig. 2. The particular features denote weaker surface yellowness, a marker of undesired scorching, degradation by light and processing (Pathare et al., 2013).

Noticeably, short-time heated MWD and RWD saffron presented similar and more homogeneous color characteristics, distinct from those of CS. Relative changes in C* and H% values (data not shown) indicated that the red color of those samples ($h^o \cong 25°$) became more vivid in a drier state implying also higher concentration of pigments. However, drying with lower microwave power intensity (MW-360) or

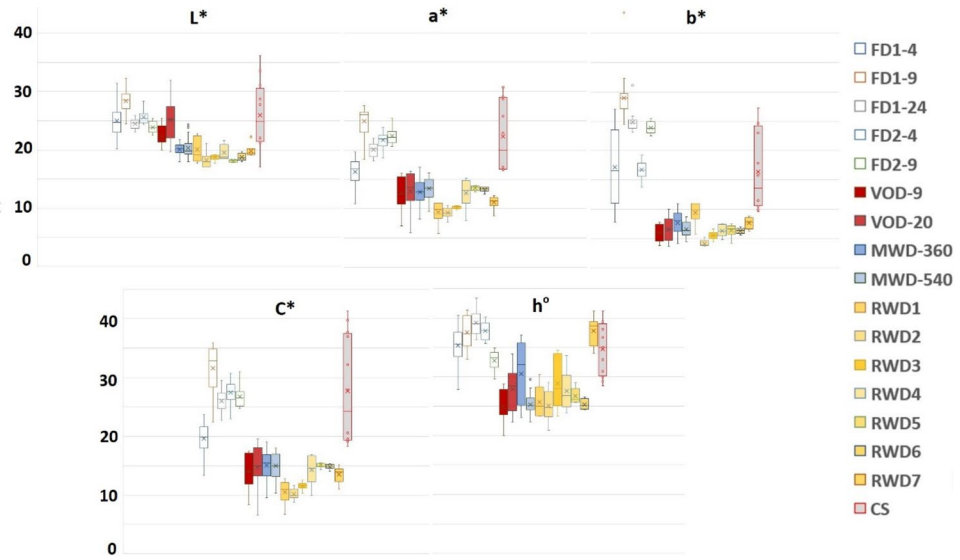


Fig. 2 Box plots representing variation in CIELAB color lightness (L*), redness (+a*), yellowness (+b*), saturation (C*), and hue (h^o) of the test samples (FD, VOD, MWD, RWD) in comparison with the control (CS). For more details about the coding, please refer to Table 1

high sample loads on a refractance window (RW1-3) caused greater variability of hue values. This profile could be associated with inhomogeneous drying or the possible formation of an outer "glassy" layer (Aguilera, 2003).

Differences in color perception due to changes in the plant cellular structure during saffron dehydration are scarcely discussed in literature. Chen et al. (2020) reported values that allow for estimation of color saturation C* and hue signifying clear discrimination of FD saffron, in line with our findings.

Compositional Variation

Color Extraction Yield

At this point, we selected samples from experiments at extreme operating conditions (sample load/MW energy/duration, etc.) to evaluate compositional variation as a measure of changes in the stigma extraction efficiency. The contents of the most valuable colorants that are sugar esters of crocetin (CRTSEs) were first assessed using the widely accepted ISO 3632-based method that is proposed for benchmarking the saffron spice products according to coloring strength, bitterness, and aroma strength (ISO, 2010). The method includes a sample preparation step that assumes grinding, exhaustive extraction, and complete recovery of CRTSEs prior to spectrophotometric estimation of specific absorption coefficient ($E^{1\%}$) values at 440 nm. The same ISO-based method proposes also measurements in the region < 300 nm to calculate the bitterness and aroma strength of the dried product as a measure of picrocrocin and safranal contents that, however, are not specific (Ordoudi & Tsimidou, 2004). In our study, the bitterness index that takes into account $E^{1\%}$ 257 values of the polar saffron extracts was regarded relevant with total contents in major non-volatile, glycosidic constituents rather than with picrocrocin. Moreover, the aroma strength evaluated using $E^{1\%}$ at 330 nm was considered as an index of the content in *cis*-isomers of CRTSEs rather than of minor contents of volatile lipophilic constituents like safranal. Figure 3a shows the trends and fluctuations of $E^{1\%}$ values at 440, 257, and 330 nm, in view also of the residual moisture (H%) and in comparison with CS.

Our results show that all the vacuum-drying or short-time heating treatments of saffron stigmas were beneficial for coloring strength, one of the most important quality characteristics of the spice. In particular, $E^{1\%}$ 440 values (285–310 a.u.) were almost 15 – 30 units higher than that of CS and tended to increase by extending exposure, more under FD rather than VOD conditions (FD1-9 and FD2-24 vs VOD-20). Previous reports also signified that short-time air-heating at 50 – 70 °C are beneficial for coloring strength (Carmona et al., 2006a, b, c).

Noticeably, MWD5-360 corresponding to the highest-sample loading treatment that required longer exposure time and overall MW energy (Online Resource 4) exhibited the highest $E^{1\%}330$ value (40 ± 2 units). Taken that MW radiation is suggested to favor the formation of *cis* crocetin esters and concomitant synthesis of safranal (García-Blázquez et al., 2021), our finding strengthens the view that MW energy input is critical for *cis/trans* isomerization reactions. As for RWD samples, different sample loadings did not affect $E^{1\%}$ 330 values that were quite lower than CS. Their $E^{1\%}$ 257 values were also low but resembled the performance of reference saffron in this case (Fig. 3a). On the other hand, FD, VOD, and MWD experiments at

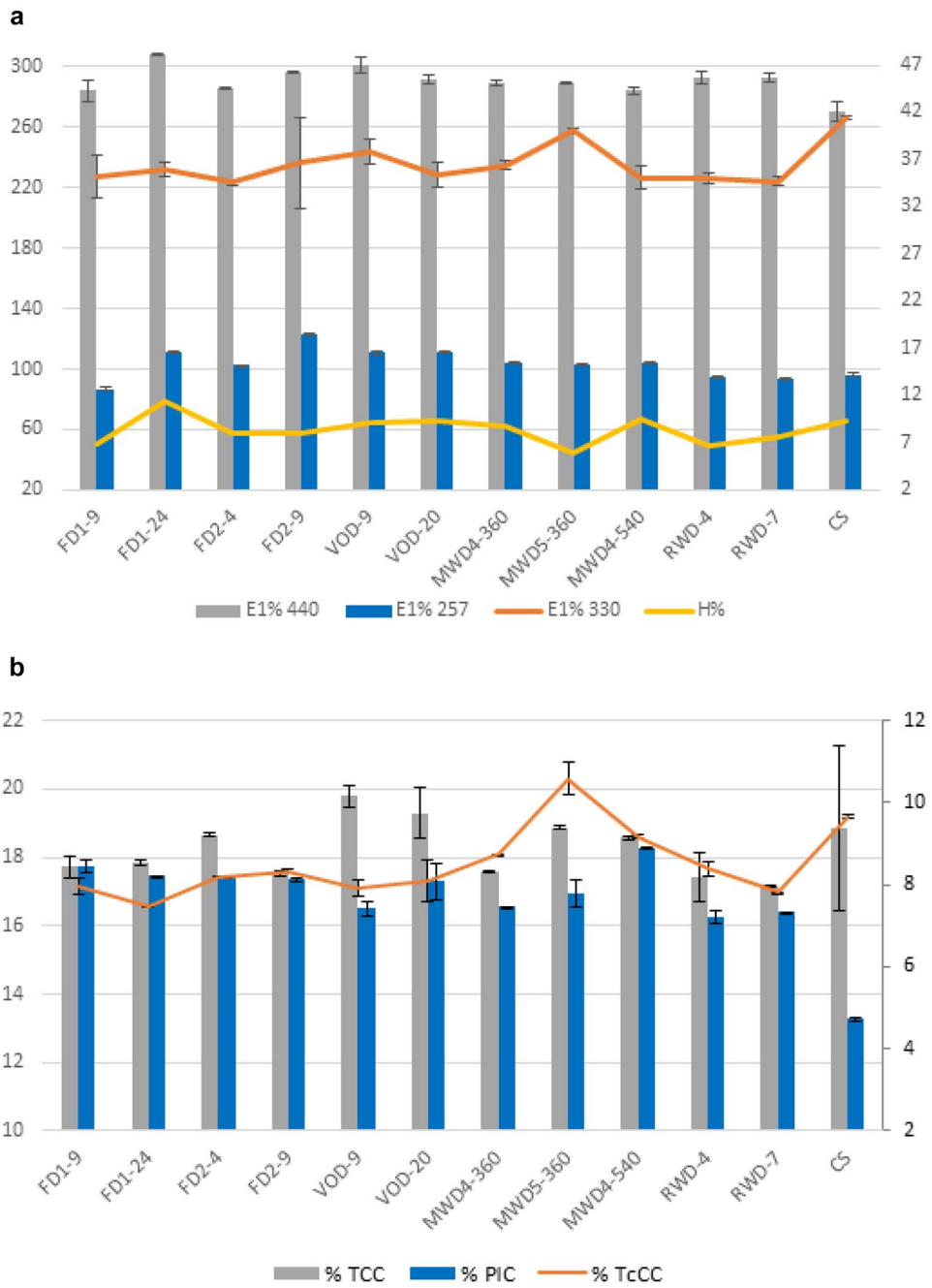


Fig. 3 **a** $E^{1\%}$ values of polar saffron extracts at 440, 257, and 330 nm, estimated by UV-Vis spectrophotometry. **b** Total % contents in crocetin sugar esters (TCC), in *cis*-crocetin sugar esters (TcCC) and picrocrocin (PIC), calculated via HPLC-DAD. Coding is according to Table 1

extreme conditions caused the bitterness index to exceed 100 a.u., an upper threshold value for traditionally dried Greek saffron samples (del Campo et al., 2010).

The UV-Vis spectrophotometric results suggest that different drying treatments imposed both positive and negative effects on the major organoleptic quality attributes of saffron stigmas. However, only by assessing the HPLC-DAD chromatographic profiles of the polar extracts at 440 or at 250 nm it became possible to attain information about the actual contents of individual constituents that could be reflected in FTIR spectral fingerprinting analyses.

HPLC-DAD Profiles

Total contents of CRTSEs (TCC in Fig. 3b) ranged widely between 16.6 and 20.4% (w/w, dw), indicating high-quality Greek saffron (Lechtenberg et al., 2008) and decreased slightly in the order VOD ≥ MWD ≥ FD ≥ RWD. Deeper insight to the chromatographic profiles and UV-Vis spectra revealed that more than 15 different polar apocarotenoid compounds were present in the extracts (Online Resource 5). Only four compounds, namely, digentiobiosyl and glucosyl-gentiobiosyl esters of all-*trans* crocetin and their 13-*cis*

isomers, accounted for > 90% of the total content in CRTSEs. Other minor peaks that most probably correspond to all-*trans* CRTSEs with higher glycosylation pattern (e.g., with neapolitanose) (Carmona et al., 2006c) accounted for about 3 – 6% of the total area of the chromatograms. It is worth stressing that VOD samples were slightly enriched in such structural analogues (up to 8% of the total area). HPLC analysis verified that microwave-dried saffron (MWD5-360, along with MW4-360 and MW5-540) was enriched in *cis*-isomers of CRTSEs, resembling CS. The processing conditions (sample load, MW power intensity) probably affected their content likewise the $E^{1\%}$ 330 values, supporting association between the two parameters, as shown in Fig. 3a, b.

The peak corresponding to picrocrocin (PIC) dominated the chromatographic profiles of all the dried samples at 250 nm (Online Resource 5). Under the tested conditions, PIC content ranged from 16.6 to 18.3% (w/w, dw) and was much higher than in CS (Fig. 3b). Such values are atypical for Greek saffron (del Campo et al., 2010; Lechtenberg et al., 2008) and verify enrichment in bitter-tasting compounds, in line with $E^{1\%}$257 data (Fig. 3a). Figure 3b shows an upward trend by intensifying the operating conditions, that is, by increasing sample loading, duration or MW energy input. Additionally, an unknown non-colored polar constituent that is eluted at $t_R = 5.1$ min and absorbs at $\lambda_{max} = 266$ nm became prominent in FD2-9 and MWD5-360 saffron extracts. Protein denaturation that favors complex interactions among the exposed amino acid residues or liberation of free organic acids from the matrix could account for this finding (Prasad et al., 2017).

Taken all these results together, it seems that saffron stigmas that were exposed at different gentle drying treatments are not differentiated based on their content in major crocetin esters or picrocrocin that define the commercial importance of the product. Variations in the contents of few, less prominent metabolites such as crocetin esters of high glycosylation pattern or *cis*-isomers are more likely to be indicative of the drying effects. The overall findings were combined to insightfully evaluate the observations from an unsupervised analysis of FTIR spectroscopic fingerprints, as discussed below.

FTIR Spectral Fingerprints

The FTIR spectra of all the test samples presented the typical peaks and bands that can be assigned to the molecular fingerprint of a pure, high-quality saffron sample (Ordoudi et al., 2014). In this case, the region between 800 and 1500 cm^{-1} bears close resemblance with the respective spectral characteristics of a lignocellulosic biomass material (Sim et al., 2012). Visual inspection of the spectra could hardly distinguish differences according to the drying treatment. Different signal pre-processing methods (normalized 0th-order and normalized 2nd-order derivative) were thus applied, first to normalize peak intensity fluctuations and then, to remove sloping effects and enhance resolution. The pre-processed data sets were co-evaluated through Principal Component Analysis (PCA) to explore grouping patterns and highlight the spectral regions and frequencies of highest importance. Biochemical relevance and mechanistic implications are discussed following a case-by-case approach, as shown in the next paragraphs.

Vacuum-Dried Saffron

Irrespective of the method of signal pre-processing four latent variables or else, principal components (PCs) were extracted from the spectra of FD saffron as they could explain > 95% of the variance in the original data. No extreme or outlying observations were found. Figure 4a depicts the allocation of FD samples according to their 1st and 4th PC score (*t*) values. The samples are labeled according to the total sample load used (2 vs 4 shelves) and colored according to the drying duration. Two clusters were formed along the 1st PC axis depending on whether the overall duration was too short (4 h) or too long (24 h). In particular, the former samples were grouped to the left part of this plot, while the latter ones were grouped to the right. Samples that were freeze-dried for 9 h did not share a grouping pattern. These data signified that variance over PC1 reflects a dynamic change in the composition of FD saffron during the last stage of dehydration. Figure 4a shows also that drier FD samples from experiments with half sample loading (2 shelves) tended to segregate in the lower (negative) part of the 4th PC, irrespective of the duration of the experiment (4 or 9 h). Time-related patterns were explored further with the aid of the variable loading (*p*) values and corresponding plots (Online Resource 6) that pinpoint the spectral features of the highest importance for each PC. For better visualization, Fig. 4b displays distinct regions of the normalized FTIR spectra of FD samples that contribute to the diagnostic PCs.

Infrared spectroscopy is particularly sensitive in hydrogen bond formation so that shifts in frequency or peak width changes as the ones depicted in Fig. 4b can be considered diagnostic of changes in water-macromolecule interactions. Above all, variance at around 3380 – 3580 cm^{-1} that is related with stretching vibration of hydrogen-bonded and non-bonded –OH groups in water molecules (Ordoudi et al., 2014) was found significant for scattering along the 1st PC. The intensities of the peaks at around 1045 – 1087 cm^{-1}, possibly due to C–O–H bending coupled to C-O and C–C stretching vibrations in mono and disaccharide molecules (Wiercigroch et al., 2017) were of minor importance. Other regions of the FTIR spectra were found significant for the scattering along the diagnostic 4th PC, e.g., bands

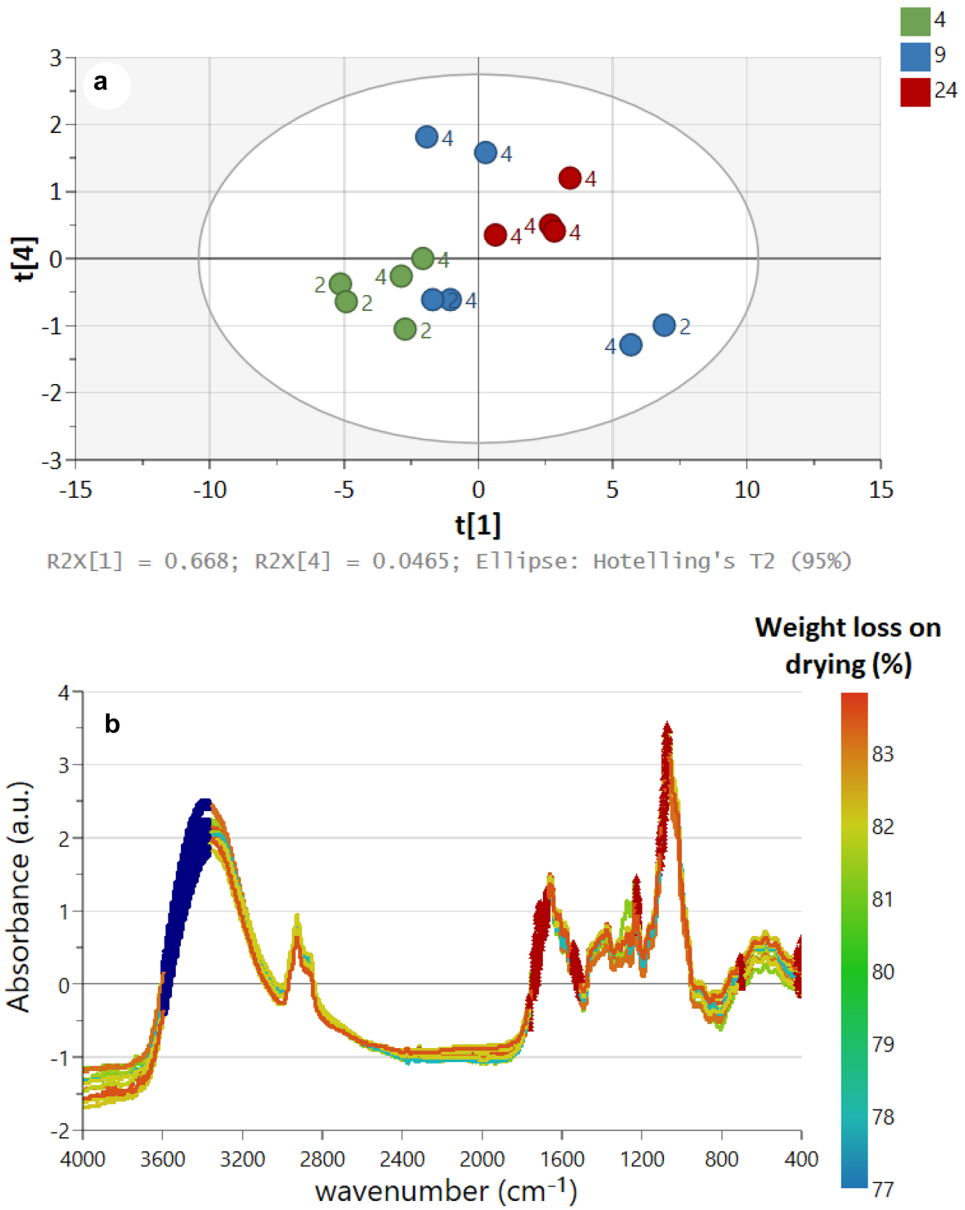


Fig. 4 **a** PCA score scatterplot and **b** normalized FTIR spectra of saffron samples from FD experiments with different drying duration (4, 9, and 24 h) and sample loading (2 or 4 shelves). Red/blue color dots denote the important spectral regions for **t**[4] and **t**[1] score distribution, respectively

in the low-frequency region between 400 – 430 cm^{-1} (possibly due to aromatic rings or -S–S- bonds) as well as between 1508 – 1550 cm^{-1} (N–H in-plane bending) and 1670 – 1750 cm^{-1} (> C = CH_2) contributed with positive **p**[4] loadings that helped to discriminate better samples from the long-duration FD experiments. On the other hand, signals at 1757 – 1764 (quite selective for -C = O, especially free and bound forms of -COOH moieties in vinyl esters and lactones), at 700 – 710 cm^{-1} (*cis* = C–H out-of-plane bending or -OH out-of-plane bending, sometimes linked to free water), and at 1220 – 1230 cm^{-1} (probably due to C(O)–O stretching in esters and –OH in-plane vibrations) had negative **p**[4] loadings, which contribute to discrimination of samples from short-duration FD experiments. Further pre-processing of the FTIR spectra through second-order derivatization (Online Resource 6) brought to attention other small regions as possible markers of compositional changes, i.e., those at around 800 and 980 – 1000 along with 1010 – 1020 cm^{-1} (-CH_2 in cyclohexane rings of sugars), 1250 – 1265 (probably due to in plane -OH vibrations), 1590 – 1600 (-NH in primary amines), 1624 – 1633 (conjugated C = C bonds, -OH bending vibration characteristic of sorbed water), and at 2852 along with 2920 cm^{-1} (-CH_2 and -CH_3 groups). The region between 1500 and 1700 cm^{-1} can be diagnostic of different interactions among proteins and ions or water upon heating at different temperatures, as it has been evidenced for cheese (Boubellouta & Dufour, 2012).

In general, it can be suggested that the spectral correlation patterns among FD saffron exposed different vibrational motions of polyunsaturated carbon chains, possibly those of

crocetin molecules, but also carboxylic esters, amino acids, lactones, or aromatic rings at the last stage of dehydration.

Diagnostic patterns according to the vacuum-drying method were also sought after compiling the data sets of FD and VOD saffron and new rounds of PCA (Online Resource 7). Stretching vibrations of O–H in hydrogen-bonded water or/and free N–H groups in amines (at around 3325 – 3470 cm^{-1}) accounted for differentiation in this case. Additionally, 2nd derivative spectral data exposed subtle differences among samples from short- and long-duration experiments, regardless of the method of drying. This was due to greater variance in the shoulder band between 1747 and 1760 cm^{-1} that can be associated with non-hydrogen bonded -COO as for example, -C=O stretching in vinyl esters or cyclic esters (lactones) or cyclic amides (lactams). It is worth mentioning that lactones, formed by the dehydration of aliphatic hydroxy acids, are also derivatives of 2(3H)-furanones which may contribute to saffron flavor (Maggi et al., 2010). The spectral variance captured by extending the duration of drying in the absence of oxygen points out the importance of this operating parameter, in line also with the discussion about increasing trend in the contents of glycosidic constituents and picrocrocin that was raised earlier (see Fig. 3a, b).

Short-Time Heated Saffron

The PCA results for rapidly dried MWD saffron indicated that the FTIR spectral data were as complex as those of FD samples. Four PCs explained sufficiently 98.4% of the original variance while 2nd-order derivatization simplified the model (3 PCs could explain 93.2% of the variance). In the former case, scattering along the 2nd PC axis, as depicted in Fig. 5a, could be associated with small variance in the drying yield (78 – 82%, w/w). Sample distribution over the 1st and 2nd PCs probably represented the combined effect of increasing sample loading (e.g., MW4-360 vs MW5-360) at varying MW power intensity (MW5-360 vs MW5-540),

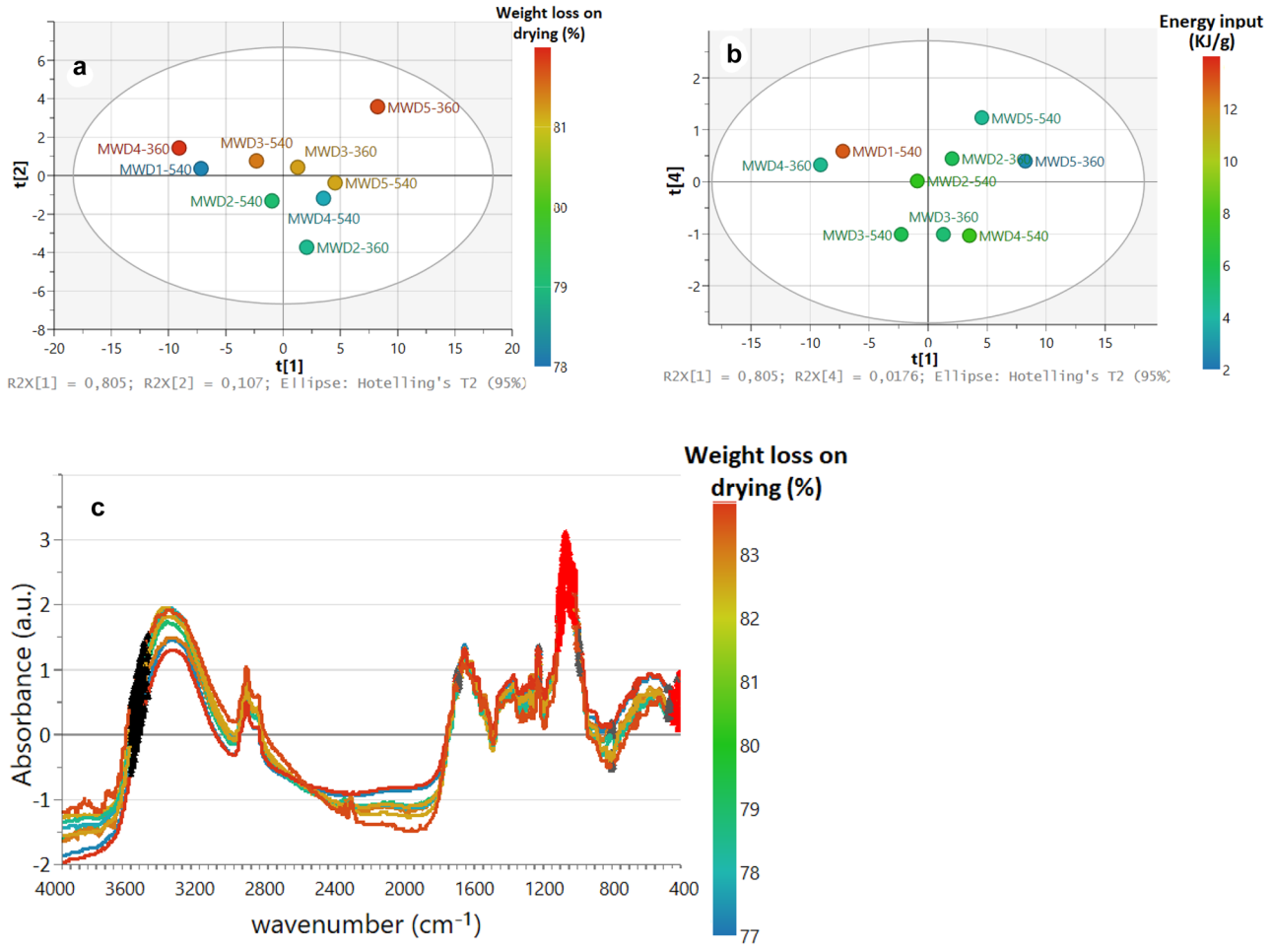


Fig. 5 PCA scatterplots of **a** t1/t2 and **b** t1/t4 score values along with **c** normalized FTIR spectra of saffron from MWD experiments. Black/red/gray dots denote important spectral regions for **t**[1], **t**[2], and **t**[4] score distribution, respectively

respectively. It is stressed again that the drier state coincided with more attractive red color but also higher content of *cis*-isomers of CRTSEs. It was noticed also that MWD samples from the high sample loading experiments at 360 and 540 W were scattered with extreme **t**[1] and **t**[4] values, respectively (Fig. 5b). The distribution pattern along the 1st PC could represent the effects of varying MW energy input. The latter are also associated with the observed variation in total CRTSEs and in picrocrocin as discussed earlier for MWD4-360 (see Fig. 2) and/or changes in the stigma surface structure (outer glassy surface) that hindered further diffusion of water and loss of volatiles from the MWD stigmas (Majumder et al., 2021; Thamkaew et al., 2021).

A large number of subtle shifts and shoulders in the spectra of MWD samples were found to account for the differential distribution on PCA scatterplots. Shifts in the region between 3520 – 3590 cm^{-1} (loaded on 1st and 3rd PC) and below 500 cm^{-1}, e.g., 410 – 427 cm^{-1} (loaded on 2nd and 3rd PC) as well as between 650 – 690 and 795 – 814 cm^{-1} (loaded on 3rd PC) could be due to changes in the vibrational modes of water complexes and interactions with inorganic anions but also due to amine, aromatic ring, or sulfur-containing bond vibrations upon prolonged treatment with lower MW energy input that resulted in higher drying yield. Several studies about the effects of microwave radiation treatment on food properties point out the possibility to modify protein secondary or tertiary structure along with weight loss. Very recently it was reported that MW treatment of heat-resistant protein-rich powder at 350 W induced partial unfolding and/or aggregation (Subasi et al., 2023). In our study, the discriminating potential of spectral features between 650–690 and 795 – 800 cm^{-1} is emphasized because they could be associated with *cis*-double bonds in aliphatic or aromatic systems (Socrates, 2004). Moreover, variance of the saccharide bands between 975 – 1005 (4th PC) and 1010 up to 1109 (2nd and 3rd PC), but also C(O)-O vibrations between 1225 – 1229 (4th PC) and 1260 – 1263 (3rd PC) and C(O) = O vibrations at 1687 – 1712 cm^{-1} (4th PC) could reflect changes in sugars that are esterified with the apocarotenoic acid moieties of CRTSEs, induced by higher MW power intensity (540W). Many other less profound spectral characteristics were revealed after 2nd-order derivatization (data not shown) that referred to intensity fluctuations at around 1736, 1672, 1647, 1560, 1535, 1508, 1450, and 1246 cm^{-1} (3rd PC). Figure 5c illustrates the regions of greater importance for the spectral patterns of MWD saffron.

Noticeably, PCA of the spectral data after refractance window drying of stigmas resulted in models of only two PCs, irrespective of the signal pre-processing method. Those simple models explained sufficiently the original variance (99.1% or 85.4% for normalized and 2nd derivative data, respectively), implying greater homogeneity in chemical composition, compared with MWD samples. The corresponding score scatterplots are illustrated in Fig. 6a and Online Resource 9. Sample distribution could be partially explained based on different sample loading. Saffron from either the lowest (300 – 400 g/m^2, RWD4-5) or the highest sample loading (750 – 900 g/m^2, RWD1-3) experiments tended to group on the right of the PCA plot with positive **t**[1] values, because of their spectral variance between 3300 and 3370 cm^{-1}. Differentiation along the 2nd PC was mainly because of -CH_2 and -CH_3 stretching vibrations subtle sharpening of bands at 2922 – 2924 cm^{-1} (Fig. 6b). The captured variance represents better the effect of high-low sample loadings or density on the refractance window and coincides with differences in surface color characteristics (see Fig. 3). Such changes could be also indicative of temperature-sensitive structural disorganization of macromolecules as a result of water removal, e.g., disorder of hydrocarbon chains and phase transition of lipids (Boubellouta & Dufour, 2012; Socrates, 2004).

The 2nd derivative spectral analysis brought to light new patterns of similarity according to the residual moisture content of the RWD samples and new bands of discriminating importance (Online Resource 9). Most of the latter were in the region below 1400 cm^{-1} (e.g., around 860, 1080, 1140 cm^{-1}) that are characteristic of skeletal vibrations of pyranose rings in saccharide moieties (Ordoudi et al., 2014). The spectral variation at around 1637 cm^{-1}, characteristic of sorbed water, was also exposed. Greater variance and shifts of about 5 – 10 cm^{-1} around 1315 and 1482 cm^{-1} may denote a significant role of -CH_2 and -CH_3 groups of hydrocarbon chains. In addition, spectral variation at around 1560, 1582, and 1618 cm^{-1} more possibly due to -COO^- moieties of free amino acids could represent heat-induced changes in polyamine groups of protein and polypeptide molecules after refractance window drying treatments. Intensity variation at 1220 and 1660 cm^{-1} that is most likely due to conjugated C = C–CO-O bond vibrations of CRTSEs (Ordoudi et al., 2014) was another feature of importance. These features unveil changes of the hydrogen bonding networks of water and sugar moieties of CRTSEs, possibly in association with proteins. Such type of interactions among the polyene chain of crocetin, sugar moieties, and β-lactoglobulin as a function of temperature were proposed recently (Allahdad et al., 2020) with unknown implications for the bio-functionality of the spice.

Diagnostic FTIR Spectral Features

All the data sets representing different drying methods were combined (FD, VOD, MW, and RW) for diagnostic feature analysis. This approach allowed for extraction of 5 PCs that explained 95.4% of the original variance ($p < 0.05$). Even so, only the distribution of scores along the 4th PC brought

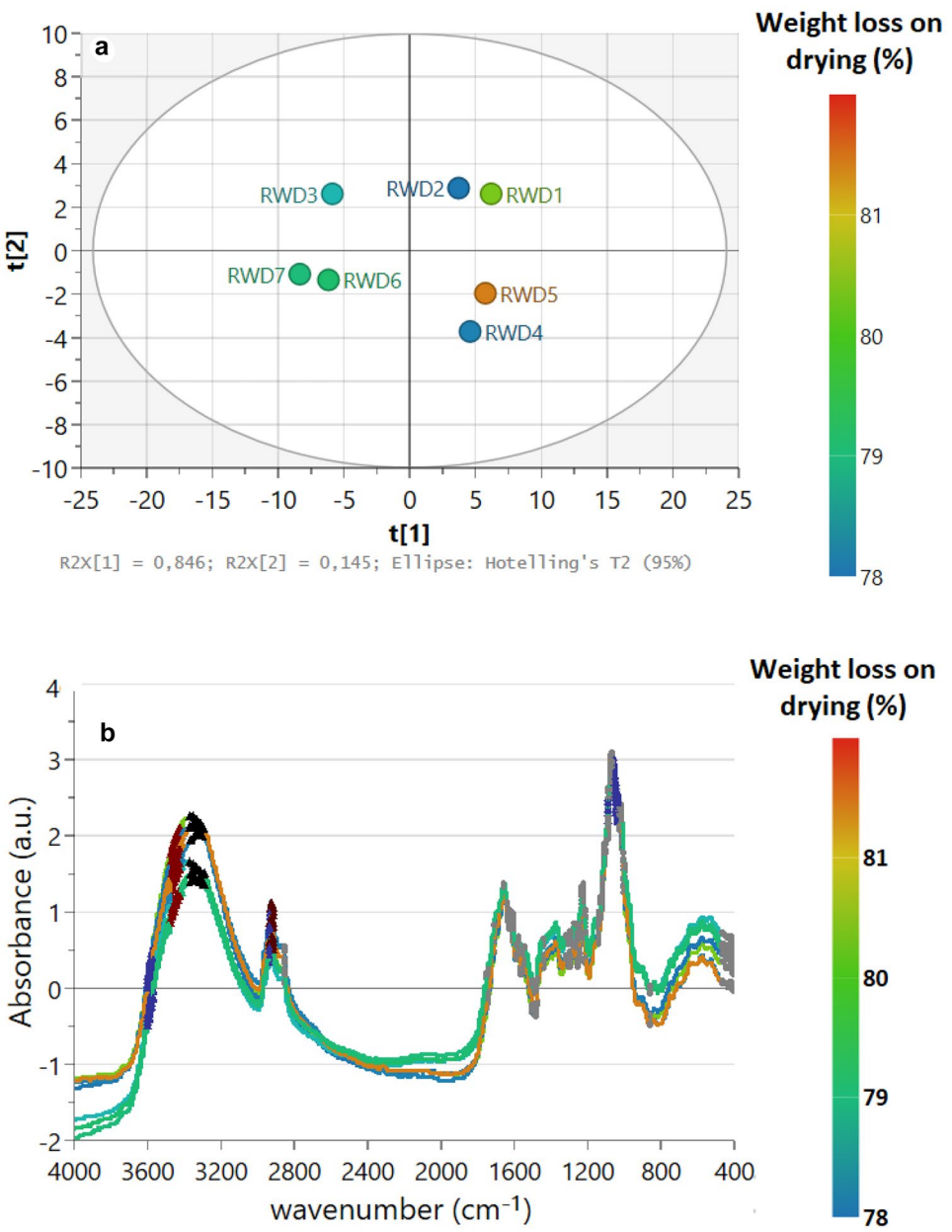


Fig. 6 **a** PCA scatterplot of **t**1/**t**2 score values and **b** normalized FTIR spectra of saffron from RWD experiments. Black/red/blue dots highlight important spectral regions that were extracted from normalized data (**t**[1], **t**[2], **t**[3], respectively), while gray dots denote the corresponding findings from 2nd derivative data analysis

information about the drying method applied, as depicted in Fig. 7a. In particular, the vacuum-dried saffron samples tended to segregate at the lower part of the PCA plot with negative **t**[4] values, separately from the short-time heated ones and irrespective of their residual moisture content. The variable loading plots indicated that changes in the sugar region between 1024 and 1150 cm^{-1} accounted for positive **p**[4] loadings. The region 1000 – 1200 cm^{-1} was then selected for further pattern recognition analysis. It was found that intensity fluctuations at ca. 1005 cm^{-1} near to the shoulder at 1016 cm^{-1} (typical of glucose residues in polysaccharides i.e. starch) as well as in the broad region between 1100 and 1200 cm^{-1} that includes the small peak at 1160 cm^{-1} (typical of C–O–C glycosidic bridges) were the reason behind the grouping pattern. Early studies of our group showed that the particular bands in the sugar region (e.g., at 1028 and 1175–1157 cm^{-1}) are diagnostic of inferior quality saffron products. The shape and intensity of the bands between 1157 and 1175 cm^{-1} are of special interest because they can expose quality deterioration due to storage (Ordoudi et al., 2014) or false "best before" claims of commercial saffron products (Consonni et al., 2016).

As a proof of concept, a test data set containing FTIR spectra of freshly harvested, high-quality saffron ($E^{1\%}$ 440 > 240 a.u.) that had been dried by their producers according to the traditional Greek practices and analyzed soon after processing was assessed. The reference samples were labeled as C1 (same batch/producer as the one used

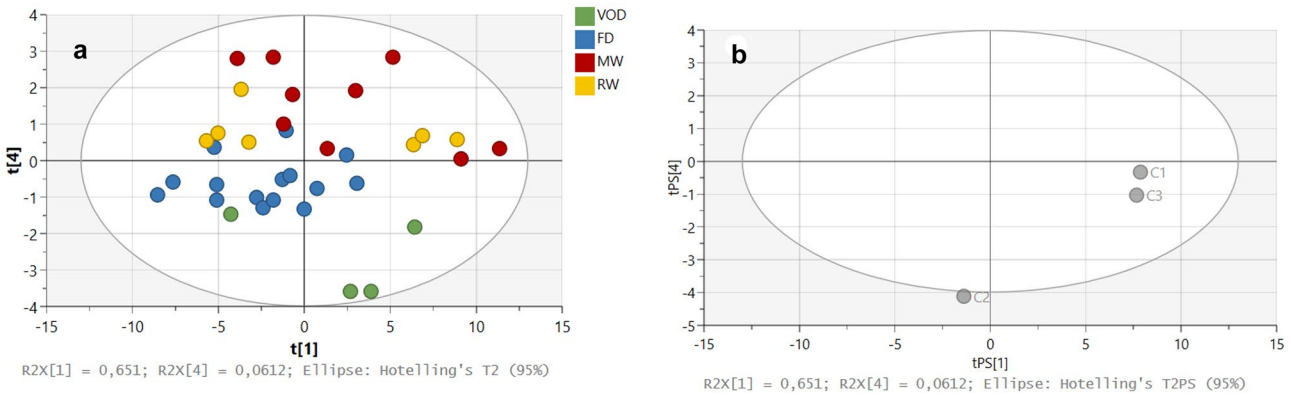


Fig. 7 PCA score plots showing the projection of **a** samples from the dehydration experiments of this study ($n = 35$) and **b** samples from freshly harvested PDO "Krokos Kozanis" samples ($n = 3$) and different batch/producer/production year

for drying experiments), C2 (2021 harvest period, second producer), and C3 (2013 harvest period, third producer). Their spectral data were projected on the PCA space modeled for FD, VOD, MWD, and RWD saffron, and the results are shown in Fig. 7b. None of the three samples was ruled out of the modeled space as outlier, a finding that points out significant similarities with saffron after non-conventional, gentle drying treatments. What is more, orthogonal projection of C1 and C3 vs C2 on the **t**[1]/**t**[4] plot with either zero or negative **t**[4] values, signifies that the particular distribution pattern was not relevant with sugar bond hydrolysis.

Conclusions

In this study, the FTIR spectra of saffron stigmas, a high-value product in the global spice trade, were thoroughly explored to unveil for the first time, possibly diagnostic patterns related with their gentle drying in vacuum or after short-time heating. Valuable insight to the physical and molecular structure transformations that took place during the last stage of stigma dehydration was gained through spectral fingerprinting, aided by exploratory Principal Component Analysis. Above all, the peak at 1160 cm^{-1} (typical of C–O–C glycosidic bridges) proved a distinguishing feature of short-time heated vs vacuum-dried saffron. Our findings highlight the novelty to combine non-destructive FTIR spectroscopy with conventional analytical techniques for more insightful investigation of saffron drying effects and evaluation of desired or undesired quality attributes. They also point out the perspective of exploiting the FTIR spectral fingerprint of this valuable raw material as a cost-effective, eco-friendly, and non-invasive solution for rapid monitoring of quality in new industrial applications.

Supplementary Information The online version contains supplementary material available at https://doi.org/10.1007/s11947-023-03119-9.

Acknowledgements The authors wish to thank the Krokos Kozanis Producers Cooperative for providing samples and technical support. They would also like to acknowledge the Interdisciplinary Laboratory of Electron Microscopy of AUTH (Greece) for providing access to SEM instrumentation and Prof. E. Pavlidou for scientific support.

Author Contribution Fotini Kokkinaki: Formal analysis, investigation, visualization, writing—original draft. Stella Ordoudi: Conceptualization, investigation, formal analysis, methodology, data curation, writing (review and editing), supervision.

Funding Open access funding provided by HEAL-Link Greece. Stella Ordoudi has received research support from Ingen. Dipl.-Ing. Agr. Christian Strunden.

Data Availability Data will be made available on reasonable request.

Declarations

Conflict of Interest The authors declare no competing interests.

Open Access This article is licensed under a Creative Commons Attribution 4.0 International License, which permits use, sharing, adaptation, distribution and reproduction in any medium or format, as long as you give appropriate credit to the original author(s) and the source, provide a link to the Creative Commons licence, and indicate if changes were made. The images or other third party material in this article are included in the article's Creative Commons licence, unless indicated otherwise in a credit line to the material. If material is not included in the article's Creative Commons licence and your intended use is not permitted by statutory regulation or exceeds the permitted use, you will need to obtain permission directly from the copyright holder. To view a copy of this licence, visit http://creativecommons.org/licenses/by/4.0/.

References

Acar, B., Sadikoglu, H., & Doymaz, I. (2015). Freeze-drying kinetics and diffusion modeling of saffron (Crocus sativus L.). *Journal of*

Food Processing and Preservation, *39*(2), 142–149. https://doi.org/10.1111/jfpp.12214

Aghaei, Z., Jafari, S. M., Dehnad, D., Ghorbani, M., & Hemmati, K. (2018). Refractance-window as an innovative approach for the drying of saffron petals and stigma. *Journal of Food Process Engineering, 41*(7), 1–9. https://doi.org/10.1111/jfpe.12863

Aguilera, J. M. (2003). Drying and dried products under the microscope. *Food Science and Technology International, 9*(3), 137–143. https://doi.org/10.1177/1082013203034640

Allahdad, Z., Khammari, A., Karami, L., Ghasemi, A., Sirotkin, V. A., Haertlé, T., & Saboury, A. A. (2020). Binding studies of crocin to β-Lactoglobulin and its impacts on both components. *Food Hydrocolloids*, *108*(April). https://doi.org/10.1016/j.foodhyd.2020.106003

Amirvaresi, A., Nikounezhad, N., Amirahmadi, M., Daraei, B., & Parastar, H. (2021). Comparison of near-infrared (NIR) and mid-infrared (MIR) spectroscopy based on chemometrics for saffron authentication and adulteration detection. *Food Chemistry*, *344*(July 2020), 128647. https://doi.org/10.1016/j.foodchem.2020.128647

Boubellouta, T., & Dufour, É. (2012). Cheese-matrix characteristics during heating and cheese melting temperature prediction by synchronous fluorescence and mid-infrared spectroscopies. *Food and Bioprocess Technology, 5*(1), 273–284. https://doi.org/10.1007/s11947-010-0337-1

Carmona, M., Zalacain, A., & Alonso, G. L. (2006a). *The chemical composition of saffron: Color, taste and aroma* (1st ed.). Editorial Bomarzo, S.L.

Carmona, M., Zalacain, A., Salinas, M. R., & Alonso, G. L. (2006b). Generation of saffron volatiles by thermal carotenoid degradation. *Journal of Agricultural and Food Chemistry, 54*(18), 6825–6834. https://doi.org/10.1021/jf0612326

Carmona, M., Zalacain, A., Sánchez, A. M., Novella, J. L., & Alonso, G. L. (2006c). Crocetin esters, picrocrocin and its related compounds present in Crocus sativus stigmas and Gardenia jasminoides fruits. Tentative identification of seven new compounds by LC-ESI-MS. *Journal of Agricultural and Food Chemistry*, *54*(3), 973–9. https://doi.org/10.1021/jf052297w

Chen, D., Xing, B., Yi, H., Li, Y., Zheng, B., Wang, Y., & Shao, Q. (2020). Effects of different drying methods on appearance, microstructure, bioactive compounds and aroma compounds of saffron (Crocus sativus L.). *LWT - Food Science and Technology*, (120), 108913. https://doi.org/10.1016/j.lwt.2019.108913

Chia-Ying, L. I., & Tian-Shung, W. U. (2002). Constituents of the pollen of Crocus sativus L. and their tyrosinase inhibitory activity. *Chemical and Pharmaceutical Bulletin*, *50*(10), 1305–1309. https://doi.org/10.1248/cpb.50.1305

Consonni, R., Ordoudi, S. A., Cagliani, L. R., Tsiangali, M., & Tsimidou, M. Z. (2016). On the traceability of commercial saffron samples using 1H-NMR and FT-IR metabolomics. *Molecules, 21*(3), 1–13. https://doi.org/10.3390/molecules21030286

del Campo, C. P., Carmona, M., Maggi, L., Kanakis, C. D., Anastasaki, E. G., Tarantilis, P. A., et al. (2010). Picrocrocin content and quality categories in different (345) worldwide samples of saffron (Crocus sativus L.). *Journal of Agricultural and Food Chemistry*, *58*(2), 1305–1312. https://doi.org/10.1021/jf903336t

García-Blázquez, A., Moratalla-López, N., Alonso, G. L., Lorenzo, C., & Salinas, M. R. (2021). Effect of Crocus sativus L. Stigmas microwave dehydration on picrocrocin, safranal and crocetin esters. *Foods*, *10*(2). https://doi.org/10.3390/foods10020404

Gregory, M. J., Menary, R. C., & Davies, N. W. (2005). Effect of drying temperature and air flow on the production and retention of secondary metabolites in saffron. *Journal of Agricultural and Food Chemistry, 53*(15), 5969–5975. https://doi.org/10.1021/jf047989j

Hassoun, A., Aït-Kaddour, A., Sahar, A., & Cozzolino, D. (2021). Monitoring thermal treatments applied to meat using traditional methods and spectroscopic techniques: A review of advances over the last decade. *Food and Bioprocess Technology, 14*(2), 195–208. https://doi.org/10.1007/s11947-020-02510-0

ISO. (2010). ISO 3632-2. Spices — Saffron (Crocus sativus L.) — Part 2 Test methods. *International Standard*.

Kanakis, C. D., Daferera, D. J., Tarantilis, P. A., & Polissiou, M. G. (2004). Qualitative determination of volatile compounds and quantitative evaluation of safranal and (HTCC) in Greek saffron. *Journal of Agricultural and Food Chemistry, 52*, 4515–4521.

Kyriakoudi, A., Ordoudi, S. A., Roldán-Medina, M., & Tsimidou, M. Z. (2015). Saffron, A Functional Spice. *Austin Journal of Nutrition & Food Sciences*, *3*(3), 1059–1.

Lechtenberg, M., Schepmann, D., Niehues, M., Hellenbrand, N., Wünsch, B., & Hensel, A. (2008). Quality and functionality of saffron: Quality control, species assortment and affinity of extract and isolated saffron compounds to NMDA and σ1 (Sigma-1) receptors. *Planta Medica, 74*(7), 764–772. https://doi.org/10.1055/s-2008-1074535

Maggi, L., Carmona, M., Sánchez, A. M., & Alonso, L. (2010). Saffron flavor: Compounds involved, biogenesis and human perception. *Functional Plant Science and Biotechnology, 4*(2), 44–55.

Majumder, P., Sinha, A., Gupta, R., & Sablani, S. S. (2021). Drying of selected major spices: Characteristics and influencing parameters, drying technologies, quality retention and energy saving, and mathematical models. *Food and Bioprocess Technology, 14*(6), 1028–1054. https://doi.org/10.1007/s11947-021-02646-7

Nindo, C. I., & Tang, J. (2007). Refractance window dehydration technology: A novel contact drying method. *Drying Technology, 25*(1), 37–48. https://doi.org/10.1080/07373930601152673

Ordoudi, S. A., de los Mozos Pascual, M., & Tsimidou, M. Z. (2014). On the quality control of traded saffron by means of transmission Fourier-transform mid-infrared (FT-MIR) spectroscopy and chemometrics. *Food Chemistry, 150*, 414–421. https://doi.org/10.1016/j.foodchem.2013.11.014

Ordoudi, S. A., Özdikicierler, O., & Tsimidou, M. Z. (2022). Detection of ternary mixtures of virgin olive oil with canola, hazelnut or safflower oils via non-targeted ATR-FTIR fingerprinting and chemometrics. *Food Control*, *142*(February). https://doi.org/10.1016/j.foodcont.2022.109240

Ordoudi, S. A., Staikidou, C., Kyriakoudi, A., & Tsimidou, M. Z. (2018). A stepwise approach for the detection of carminic acid in saffron with regard to religious food certification. *Food Chemistry, 267*, 410–419. https://doi.org/10.1016/j.foodchem.2017.04.096

Ordoudi, S. A., & Tsimidou, M. Z. (2004). Saffron quality: Effect of agricultural practices, processing and storage. In R. Dris & S. M. Jain (Eds.), *Production Practices and Quality Assessment of Food Crops Volume 1* (Vol. 1, pp. 209–260). Kluwer Academic Publishers. https://doi.org/10.1007/1-4020-2533-5_8

Pathare, P. B., Opara, U. L., & Al-Said, F. A. J. (2013). Colour measurement and analysis in fresh and processed foods: A review. *Food and Bioprocess Technology, 6*(1), 36–60. https://doi.org/10.1007/s11947-012-0867-9

Petrakis, E. A., Cagliani, L. R., Tarantilis, P. A., Polissiou, M. G., & Consonni, R. (2017). Sudan dyes in adulterated saffron (Crocus sativus L.): Identification and quantification by 1H NMR. *Food Chemistry, 217*, 418–424. https://doi.org/10.1016/j.foodchem.2016.08.078

Prasad, S., Mandal, I., Singh, S., Paul, A., Mandal, B., Venkatramani, R., & Swaminathan, R. (2017). Near UV-Visible electronic absorption originating from charged amino acids in a monomeric protein. *Chemical Science, 8*(8), 5416–5433. https://doi.org/10.1039/c7sc00880e

Ren, Y., Lin, X., Lei, T., & Sun, D. W. (2022). Recent developments in vibrational spectral analyses for dynamically assessing and monitoring food dehydration processes. *Critical Reviews in Food*

Science and Nutrition, 62(16), 4267–4293. https://doi.org/10.1080/10408398.2021.1947773

Sim, S. F., Murtedza, M., Mohd Irwan, Lu., & N. A. L., Sarman, N. S. P., & Samsudin, S. N. S. (2012). Computational FTIR with PCA. *BioResources, 7*(4), 5367–5380.

Socrates, G. (2004). *Infrared and Raman characteristic group frequencies*. (G. Socrates, Ed.) (3rd ed., Vol. 35). Chichester: John Wiley and Sons, Ltd. https://doi.org/10.1002/jrs.1238

Subasi, B. G., Yildirim-Elikoglu, S., Altin, O., Erdogdu, F., Mohammadifar, M. A., & Capanoglu, E. (2023). Non-thermal approach for electromagnetic field exposure to unfold heat-resistant sunflower protein. *Food and Bioprocess Technology, 16*(2), 313–326. https://doi.org/10.1007/s11947-022-02929-7

Thamkaew, G., Sjöholm, I., & Galindo, F. G. (2021). A review of drying methods for improving the quality of dried herbs. *Critical Reviews in Food Science and Nutrition, 61*(11), 1763–1786. https://doi.org/10.1080/10408398.2020.1765309

Tsimidou, M., & Biliaderis, C. G. (1997). Kinetic studies of saffron (Crocus sativus L.) quality deterioration. *Journal of Agricultural and Food Chemistry*, *45*(8), 2890–2898. https://doi.org/10.1021/jf970076n

Wiercigroch, E., Szafraniec, E., Czamara, K., Pacia, M. Z., Majzner, K., Kochan, K., et al. (2017). Raman and infrared spectroscopy of carbohydrates: A review. *Spectrochimica Acta - Part a: Molecular and Biomolecular Spectroscopy, 185*(October), 317–335. https://doi.org/10.1016/j.saa.2017.05.045

Zalacain, A., Ordoudi, S. A., Díaz-Plaza, E. M., Carmona, M., Blázquez, I., Tsimidou, M. Z., & Alonso, G. L. (2005). Near-infrared spectroscopy in saffron quality control: Determination of chemical composition and geographical origin. *Journal of Agricultural and Food Chemistry*, *53*(24). https://doi.org/10.1021/jf050846s

Publisher's Note Springer Nature remains neutral with regard to jurisdictional claims in published maps and institutional affiliations.